Journal of Mining and Environment (JME) Vol. 15, No. 4, 2024, 1563-1577

Shahrood University of Technology

Journal of Mining and Environment (JME)

Journal homepage: www.jme.shahroodut.ac.ir

Iranian Society of Mining Engineering (IRSME)

Application of Fractal Modeling for Accurate Resources Estimation in the Qarah Tappeh Copper Deposit, NW Iran

Sepideh Ghasemi, Ali Imamalipour*, and Samaneh Barak

Department of Mining Engineering, Faculty of Engineering, Urmia University, Urmia, Iran

Article Info

Received 13 September 2023
Received in Revised form 7 April 2024
Accepted 12 April 2024
Published online 12 April 2024

DOI: 10.22044/jme.2024.13601.2513

Keywords

Fractal
Reserve estimation
Ordinary kriging
Micromine
Qarah Tappeh copper deposit

Abstract

This investigation centers on the Qarah Tappeh copper deposit, situated in the northern region of West Azerbaijan province, approximately 15 kilometers northeast of Maku city. The primary objective of the study is to comprehensively examine the study area through the analysis of 253 lithogeochemical samples, and assessing reserves utilizing ordinary kriging, guided by subsurface data obtained from 14 boreholes totaling 909.2 meters. The concentration–volume (C–V) multifractal modeling approach was employed to estimate the deposit's reserve. The findings of this research project indicate an estimated 988,604 tons of the deposit with an average grade of 0.14%. Through the analysis of log–log plots within the C–V relationship, threshold values signifying various copper (Cu) concentrations were identified. These plots revealed a pronounced power-law correlation between Cu concentrations and their corresponding volumes, with arrows denoting four specific threshold values. Utilizing this analytical methodology, mineralized zones were classified into five distinct categories: high (>0.42%), above-average (0.35-0.42%), average (0.27-0.35%), below-average (0.14-0.27%), and low (<0.14%) mineralized zones.

1. Introduction

In an inaugural demonstration, [1] delineated the emergence of a fractal relationship between the accumulation reserve in a field and the average grades across its distinct components. [2] investigated and unveiled a fractal correlation between grades, element concentrations, and the geometric characteristics of their geochemical distribution. Various fractal methods, such as grade-area, power-spectrum-area, grade-distance, and grade-number methods [3-10] have been employed for geochemical exploration and anomaly detection. [11] scrutinized the correlation between geological models and grade-volume fractals, affirming the accuracy of interpretations based on the caliber-volume fractal model. The study by [12] centered on characterizing mineralized zones employing a grade-volume fractal model, specifically assessing the influence of simple kriging and simple multi-Gaussian estimation techniques on iron reserves. They implemented the grade-volume fractal model on underground data to evaluate its efficacy. Additionally, various researchers [13-18] have utilized fractal methods in their studies.

[19] explored the geothermal potential in Ardabil, introducing the 'de-fractal spectral depth' method, which utilizes fractal analysis to analyze magnetic source depths from aeromagnetic data in the Ardebil province, revealing variable depths (ranging from 10.4 km to 21.1 km) and fractal parameters (ranging from 3.7 to 4.5). [20] delved into gold mineralization in Zarshuran, utilizing the Concentration-Area (C-A) fractal model to correlate gold mineralized stages with geological findings. [14] compared methods for geochemical anomaly detection, favoring the Spectrum-Area (S-A) fractal model, which applies fractal analysis to geochemical data for improved anomaly identification, particularly effective in complex geological settings. [21] investigated ore grade

* Corresponding author: a.imamalipour@urmia.ac.ir (A. Imamalipour)

estimation and alteration zone delineation employing the Wavelet Neural Network (WNN), a methodology that integrates wavelet theory and Artificial Neural Network (ANN), surpassing Ordinary Kriging (OK) in overall accuracy. [22] detected iron oxide alteration zones in the Tarom region using satellite data and the Spectrum-Area (S-A) fractal model, which utilizes fractal analysis to delineate alteration zones based on spectral characteristics. Lastly, [23] mapped contamination around Irankuh Pb–Zn mine utilizing Principal Component Analysis (PCA) integrated with Concentration-Area (C-A) and Spectrum-Area (S-A) fractal models, effectively identifying pollution anomalies by analyzing the spatial distribution of contaminants with fractal-based methods.

The advent of Micromine software in (1986) has significantly revolutionized 3D exploration and design of open pit and underground mines, offering a comprehensive toolset for detailed project design and management. Noteworthy applications of Micromine software include simulation of the economic transportation system for the Haji-Abad Bukan mine [24], determination of grades and optimal production planning for the Qalqele gold mine [25], and geological and block modeling efforts for the Qarah Qeshlaq marble deposit [26].

Kriging, named in honor of D. Craig, a mining engineer, has been a cornerstone in geostatistical estimation. [27] utilized ordinary kriging for estimating reserves in the central part of the northern anomaly of Ahan Chagharat, revealing an absence of anisotropy in iron storage across different directions. [28] employed normal kriging and index kriging methods, underscoring that the standard errors of index kriging were more intricately related to estimation errors than those of normal kriging.

[29] correlated induced polarization, electrical resistivity, and copper grade at Abassabad copper mine using geophysical profiles and borehole data. Geostatistical methods produced two- and three-dimensional ore distribution models. Employing artificial neural network and cokriging methods, they predicted copper ore presence, reducing borehole requirements by 45% and optimizing drilling locations for efficient exploration.

[30] employed a hybrid methodology integrating drilling and IP-Rs data for mineral resource estimation. The analysis, utilizing statistical and geostatistical techniques, including regression, multivariate regression analysis, and cokriging, revealed that regression analysis of the correlation between IP data and copper (Cu) grade produced a more accurate model with minimized errors. This underscores the effectiveness of using IP data for precise Cu grade estimation in mineral resource assessment.

The exploration of the McArthur lead and zinc mine in northern Australia in (2001) by Pearly demonstrated the efficacy of the inverse distance method and the subsequent normal greeching method, with the latter proving more effective. [31] employed geostatistics and fractals to estimate the reserves of the Gian Buwanat copper deposit. Notably, the use of normal creaking methods, index creaking simulation, and fractal sequential arc simulation revealed the superior performance of the fractal method in comparison to the other two approaches.

[32] contributed by presenting a kinetic model for leaching in an ammonia environment, determining an activation energy of 16 kJ/mol. Their comparative analysis of acid and ammonia leaching methods for the Qarah Tappeh copper oxide ore favored ammonia leaching as the most suitable method for dissolving copper from this particular ore.

[33] emphasized the significance of structural factors such as faults, fractures, stratigraphic control, and reduction conditions in the host rock for controlling mineralization. While proposing a microdiorite-composite sill intrusion as a potential source of copper in the Permian carbonate host rock, the study considered alternative scenarios, including the possibility of copper transportation by saline waters and subsequent deposition under favorable conditions. Microscopic and field studies suggested parallels with the Kipushi copper-zinc deposit in Congo.

[34] focused on identifying sulfidic mineralized zones in the QarahTappeh (The case study of this research) Cu deposit in NW Iran using geo-electrical data and fractal models. Their study revealed a high sulfidic mineralized zone in the NW area, emphasizing the effectiveness of multifractal modeling for optimizing mineral exploration operations and proposing grid drilling in the detailed exploration stage.

This research undertook a comprehensive evaluation of anisotropic copper deposit reserves, employing conventional kriging, fractal analysis, classical triangulation, and 3D modeling through Micromine software. Significantly, the results highlighted the superior performance of fractal simulation in accurately simulating the low thickness and discontinuities of the Maku Qarah Tappeh copper deposit following geological features, surpassing the efficacy of other methods. This collective body of research underscores the

evolving methodologies in mineral exploration, offering valuable insights into the intricate dynamics of reserve estimation across diverse geological settings.

2. Geological setting

The surveyed mining region is situated in Maku city, within the North of the West Azerbaijan province, Iran (the intersection of the Alborz-Azerbaijan structural earth zone and Urumieh-Dokhtar Cenozoic magmatic belt). Geological mapping at a scale of 1:5000 reveals the presence of rock formations belonging to four distinct sedimentary sequences, originating from varying geological periods. These sequences, arranged chronologically from oldest to most recent, encompass the Permian, Oligocene, Lower Miocene, Upper Miocene, and Quaternary periods [35]. The principal lithological constituents of this deposit comprise limestone, dolomite, and diabasic dykes. Ore minerals encompass chalcocite, malachite, azorite, bornite, cuprite, and tenorite. The mineralization in the region is notably influenced by numerous faults and fractures. Additionally, silicification is evident within the deposit [34].

The Permian rock units comprise a succession of carbonate rocks, encompassing limestone, dolomitic limestone, marly limestone, and dolomite. Moving upwards in the stratigraphic sequence, the Oligocene rock units consist of nummulitic limestone, calcareous conglomerate, sandy limestone, and sandstone, with discontinuous and angular occurrences observed on the Permian formations. Notably, a destruction complex, distinguished by its red coloration due to iron oxide abundance, is present on the Oligocene rock units, composed of sandstone, siltstone, and mudstone. The Upper Miocene period introduces rock units discontinuously overlaying older formations, primarily observed in the southern margins of the study area. Quaternary alluvial sediments extensively cover a substantial portion of the exposed rock outcrops [35].

Within the studied region, sporadic outcrops of diabase dykes are discernible, often associated with ore-rich areas. Initially dark gray when fresh, these dykes undergo alteration, manifesting hues of red, yellow, and orange contingent upon the formed compounds. Despite their modest dimensions, these dykes appear to exert a significant influence on mineralization processes. Microscopic examination identifies these dykes as predominantly of diabase type, characterized by coarse crystals of plagioclase and pyroxene, occasionally accompanied by olivine. The phytic texture is evident in the mineral field, with notable alterations, including chlorite, carbonate, and clay transformations [35].

From a tectonic perspective, the paramount structural features in the mapped area are faults, instrumental in shaping the morphological characteristics, inducing alteration, and influencing mineralization patterns. Mineralization examination highlights a predominant association with reverse faults, frequently delineating the boundaries between dolomitic limestone and marl limestone. The dolomite limestone horizons, due to their permeability and porosity, create a conducive environment for mineralization, in contrast to the less permeable marl horizons that impede the expansive spread of mineral constituents [35]. Figure 1 illustrates the detailed geological map, featuring prominent fault lines within the study area.

The copper mineralization found in Qarah Tappeh Maku represents a relatively rare deposit type that is less commonly identified in other global locations. While extensive gold mineralization in carbonate rocks, such as Carlin and pseudo-Carlin type deposits, is quite common, copper mineralization in carbonate rocks is less frequently encountered. Specifically, the type of copper mineralization observed in Qarah Tappeh Maku occurs within carbonate horizons and manifests as epigenetic and strataband mineralizations. This mineralization closely resembles manto-type deposits, where the host rock is primarily carbonate. It is noteworthy that in the manto-type deposits, the host rock typically consists of volcanic material, distinguishing it from the observed copper mineralization in Qarah Tappeh Maku, where the exclusive host rock is carbonate in nature. This unique geological characteristic sets the copper mineralization in Qarah Tappeh Maku apart, contributing to its distinctive identity within the spectrum of global copper deposits. The visual depiction captures the outcrop scene characterized by veined and dispersed copper oxide mineralization within the mineralized area as depicted in Figure 2.

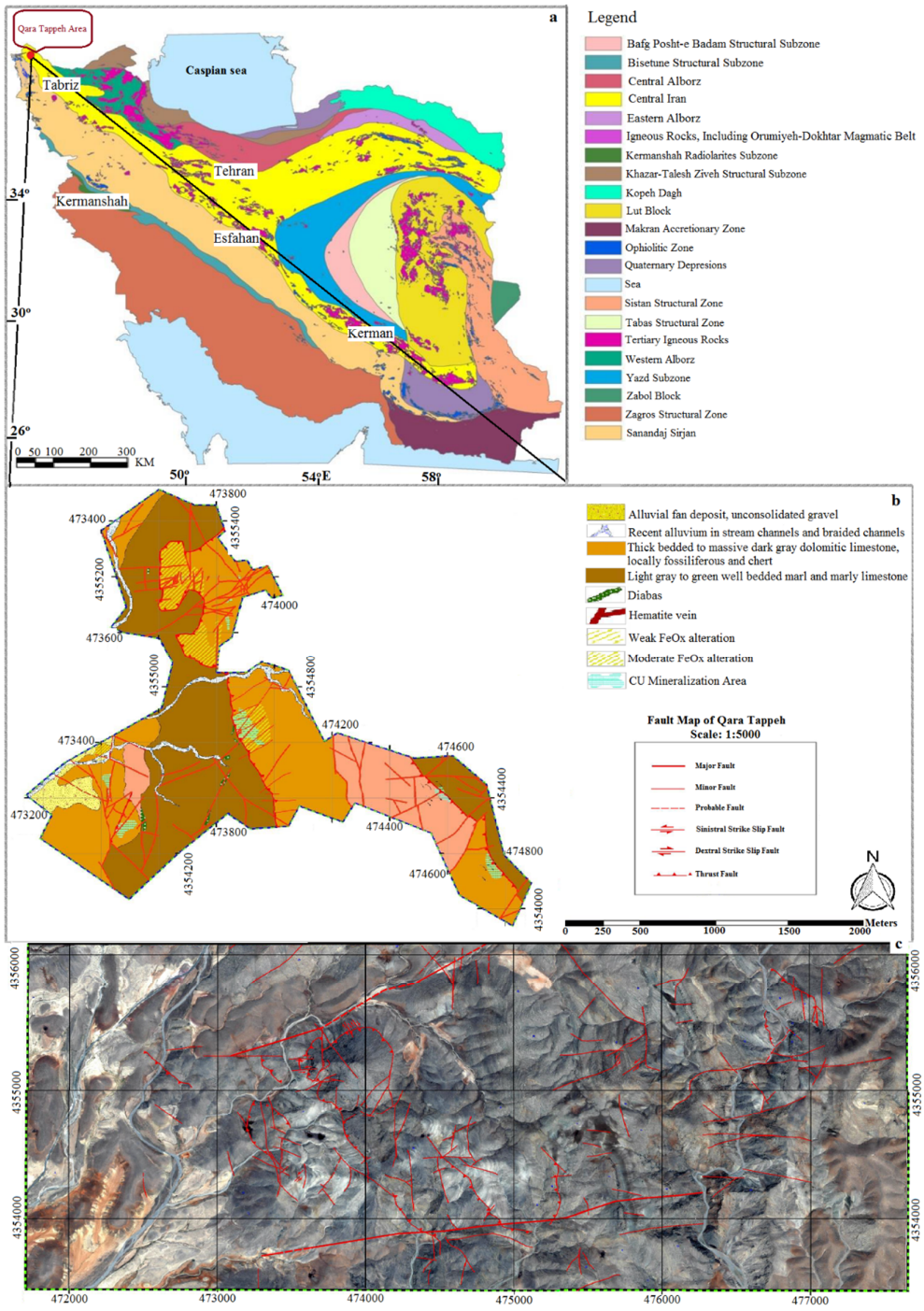

Figure 1. Major tectonic trends in Iran [36], location of study area (Qarah Tappeh copper deposit) in northwestern Iran (a), the detailed geological map (1:1000) (b), and prominent fault lines within the study area (c) [35].

Figure 2. Vein-veinlet mineralization of copper oxide mineralization in the studied deposit within the mineralized area [35].

3. Materials and methods

A comprehensive set of 253 lithogeochemical samples was employed for analysis within the specified region. The data collection was systematically conducted on a grid with dimensions of 90*90 meters along east-west profiles. Analysis of the collected data was carried out utilizing an ICP (Inductively Coupled Plasma) device, facilitated by the expertise of the [35].

To supplement the lithogeochemical analysis, exploratory drilling through coring was implemented. A total of 14 boreholes were strategically positioned, collectively spanning a distance of 909.2 meters. This drilling approach aimed to provide a more in-depth understanding of the geological features and mineral composition within the surveyed area.

Classical methods for reserve estimation, such as the section method, triangle method, and polygon method, rely on assumptions of mineral material continuity, linear thickness variability, or variability based on the radius of equal influence. These methods utilize grade and average specific weight for each geological unit [37]. Univariate statistical methods form the basis of any geochemical study with a statistical orientation. Following a pre-statistical process, both univariate and multivariate methods, including Pearson correlation, fractal analysis, and dendrogram, were employed. Table (1) provides descriptive statistics extracted from IBM SPSS (version 22), and all data were normalized by the Cox Box technique, before applying statistical methods. The normalization process is visually represented through qq plots and histograms for the copper element in Figure 3.

Kriging, a geostatistical estimation method, operates on the principle of a weighted moving average. It enables the estimation of mineral piece grades using sample grades within or outside the piece [38]. Micromine software serves as a comprehensive and user-friendly tool for 3D exploration and design of both open pit and underground mines. This software's toolkit allows for the detailed modeling and management of all aspects of mining projects. Notably, [39] demonstrated the effective use of Micromine software in creating comprehensive models to communicate mining projects efficiently to stakeholders. In the subsequent analysis, the demarcation of the mineralized zone within the study area was executed using the fractal concentration-volume (C-V) methodology [40]. This model serves as a systematic framework for delineating discrete mineralization zones, with the primary objective of mapping the spatial distribution of major, minor, and trace element concentrations within the Iranian copper porphyry deposits, notably the Sungun and Chah-Firuzeh deposits. The model is defined by the ensuing generic expression:

$V(\rho \leq \upsilon) \propto \rho^{-a1}$; $V(\rho \geq \upsilon) \propto \rho^{-a2}$

In this context, the symbols $V(\rho \leq \upsilon)$ and $V(\rho \geq \upsilon)$ signify volumes (V) associated with concentration values (ρ) that are below and above designated contour values (υ). These contour values delineate the respective volumes, with a1 and a2 serving as exponents in the mathematical representation. When examining log–log plots illustrating concentration contours against volumes, specific concentration contours are identified as threshold values. These contours, identified as breakpoints in the plots, play a crucial role in segregating geochemical populations within the dataset [40].

Table 1. Descriptive statistics of the elements in the study area.

	Minimum	Maximum	Mean	Std. Deviation	Variance	Skewness	Kurtosis
Ag	0.38	9.97	1.28	1.66	2.77	3.28	13.62
Al	0.08	7.46	1.00	1.43	2.03	3.06	9.72
As	16.60	76.86	17.69	8.13	66.03	7.42	55.00
Be	0.28	0.61	0.30	0.06	0.00	3.53	16.34
Ca	9.40	24.86	19.32	3.97	15.74	-1.06	0.58
Cd	0.78	0.78	0.78	0.00	0.00	.	.
Ce	4.04	12.94	4.51	1.74	3.03	3.99	15.65
Co	3.81	32.96	5.09	4.27	18.22	5.57	34.93
Cr	3.76	33.48	6.59	6.24	38.96	3.30	11.46
Cu	14.35	11908.50	2617.14	2870.56	8240101.38	1.43	1.78
Fe	0.08	3.05	0.28	0.42	0.17	5.76	37.78
K	0.08	3.85	0.55	0.71	0.51	3.08	10.25
La	2.82	17.56	3.58	2.74	7.49	4.04	16.61
Mg	6.63	10.65	8.59	0.63	0.40	0.72	3.76
Mn	0.00	5918.15	822.30	1025.37	1051377.73	3.34	12.99
Mo	0.76	20.51	3.32	4.07	16.53	2.88	9.84
Na	0.20	9.72	1.61	2.04	4.14	2.79	7.35
Ni	3.75	3.75	3.75	0.00	0.00	.	.
P	0.01	1.77	0.09	0.24	0.06	6.60	46.53
Pb	3.77	124.22	19.33	21.88	478.78	3.09	11.05
S	0.05	11.17	0.64	1.49	2.21	6.85	49.18
Sb	4.33	149.37	27.40	28.70	823.54	2.51	7.36
Sr	50.30	761.07	150.42	120.33	14480.48	3.43	13.83
Ti	0.01	0.66	0.02	0.09	0.01	7.20	52.71
V	3.83	173.26	29.18	22.87	523.24	4.98	30.04
Y	3.75	18.13	4.53	2.82	7.97	3.98	15.67
Zn	7.64	54.27	13.28	9.56	91.42	2.49	6.83
Zr	7.64	293.91	39.52	52.36	2741.89	3.31	12.00

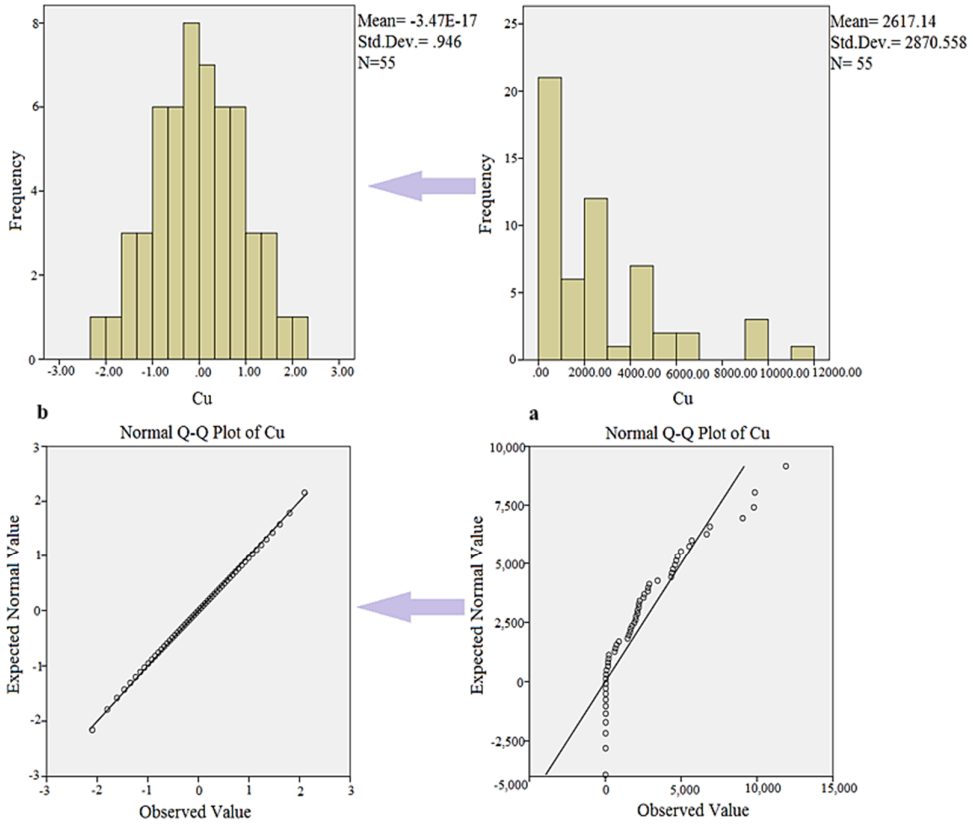

Figure 3. The distribution function before normalization (a), and the distribution function after the normalization process (b).

4. Results and discussion

4.1. Multivariate techniques

The examination of multi-element geochemical relationships involves the application of diverse multivariate statistical methods, including cluster analysis (dendrogram), correspondence analysis, discriminant analysis, factor analysis, regression analysis, principal component analysis, etc. [41]. In this statistical approach, the random errors of one variable can be partially mitigated by the inclusion of other variables. This can prove effective and beneficial, particularly in minimizing abnormal errors during data analysis and facilitating more realistic inferences [38].

Initially, the multivariate technique applied is factor analysis, wherein the aim is to reduce the number of obtained variables while retaining the essential information from the main variables. To identify a set of elements within a group, elements with high factor scores (typically exceeding 0.6) should be chosen in each column and categorized into a single group [38, 42]. The factor analysis of the range provides the following outcomes, taking into account Table (2):

First Factor: K, Mn, Mo, Na, Pb, Sb, Sr, Zr, Al, Be, Ca

Second Factor: Ce, Co, Cr, La, Ti, Y

Third Factor: Cu, P

Fourth Factor: S

Fifth Factor: Be

Sixth Factor: Mg

Seventh Factor: V

In the context of factor analysis, placing Cu and P elements in a paragenesis group indicates a significant association or co-occurrence between these elements. They tend to exhibit similar patterns or behaviors (paragenesis group) within the studied geological context. This grouping suggests a potential geological or mineralogical correlation between Cu and P in the studied area.

Table 2. The outcomes of the factor analysis method applied to the study area

Variable (ppm)	Factor 1	Factor 2	Factor 3	Factor 4	Factor 5	Factor 6	Factor 7	Factor 8	Factor 9	Factor 10
Ag	0.31	0.15	0.18	-0.02	-0.04	0.01	-0.01	-0.91	0.07	-0.01
Al	**0.77**	0.48	0.21	-0.19	-0.14	0.08	-0.20	-0.09	0.02	-0.02
As	-0.11	-0.01	-0.08	0.05	**0.98**	0.04	-0.01	0.03	-0.01	0.02
Be	**-0.77**	0.49	-0.23	0.01	0.10	0.05	-0.11	0.09	0.09	0.15
Ca	**0.86**	-0.11	0.31	-0.02	-0.04	-0.10	-0.12	-0.01	-0.10	0.08
Ce	0.18	**0.96**	0.09	0.07	0.00	0.03	0.00	-0.06	0.00	-0.07
Co	0.18	**0.89**	0.06	-0.13	-0.02	0.16	-0.25	-0.06	0.19	-0.01
Cr	0.47	**0.71**	0.04	-0.27	0.01	-0.07	-0.09	-0.19	0.24	-0.12
Cu	0.37	0.12	**0.86**	-0.08	-0.05	0.08	-0.15	-0.12	0.06	-0.06
Fe	0.40	0.59	0.25	-0.10	0.31	0.20	-0.42	0.00	0.22	0.10
K	**0.79**	0.47	0.18	-0.22	-0.11	0.08	-0.13	-0.12	0.04	-0.08
La	0.18	**0.97**	0.05	0.03	0.00	0.04	-0.03	-0.05	-0.01	-0.05
Mg	0.04	-0.19	-0.10	0.07	-0.05	**-0.96**	0.05	0.01	0.06	0.00
Mn	**0.87**	0.23	0.25	-0.15	0.00	0.11	-0.21	-0.07	-0.10	-0.04
Mo	**0.69**	0.20	0.17	-0.18	-0.03	-0.09	-0.03	-0.25	0.42	-0.16
Na	**0.83**	0.37	0.05	-0.23	-0.15	-0.13	-0.05	-0.15	0.04	-0.15
P	0.35	0.10	**0.74**	-0.42	-0.06	0.16	-0.10	-0.12	0.08	0.06
Pb	**0.76**	0.34	-0.04	-0.02	0.22	0.16	0.08	-0.12	0.35	-0.12
S	0.36	0.03	0.26	**-0.86**	-0.06	0.08	-0.04	-0.01	0.02	-0.03
Sb	**0.62**	0.13	0.03	-0.04	-0.04	0.01	-0.04	-0.01	0.08	**-0.75**
Sr	**0.81**	0.48	0.09	-0.07	0.06	-0.03	-0.11	-0.14	0.10	-0.15
Ti	0.12	**0.90**	0.10	-0.14	-0.02	0.14	-0.24	-0.02	0.15	0.05
V	0.25	0.48	0.25	-0.05	0.00	0.06	**-0.78**	-0.01	-0.01	-0.05
Y	0.18	**0.97**	0.07	0.04	0.00	0.04	-0.02	-0.06	-0.01	-0.05
Zn	-0.02	0.45	0.52	0.00	-0.05	-0.19	-0.03	-0.12	**0.61**	-0.06
Zr	**0.79**	0.51	0.07	-0.19	-0.09	0.06	-0.08	-0.13	0.07	-0.12

In the cluster analysis method, the objective is to establish a criterion for classifying variables or samples with maximum intra-group similarity and inter-group difference. Using SPSS software, a dendrogram was generated for the geochemical data of the Qarah Tappeh area (Figure 4). The ward method was employed for clustering, and the block method was utilized for measuring distances.

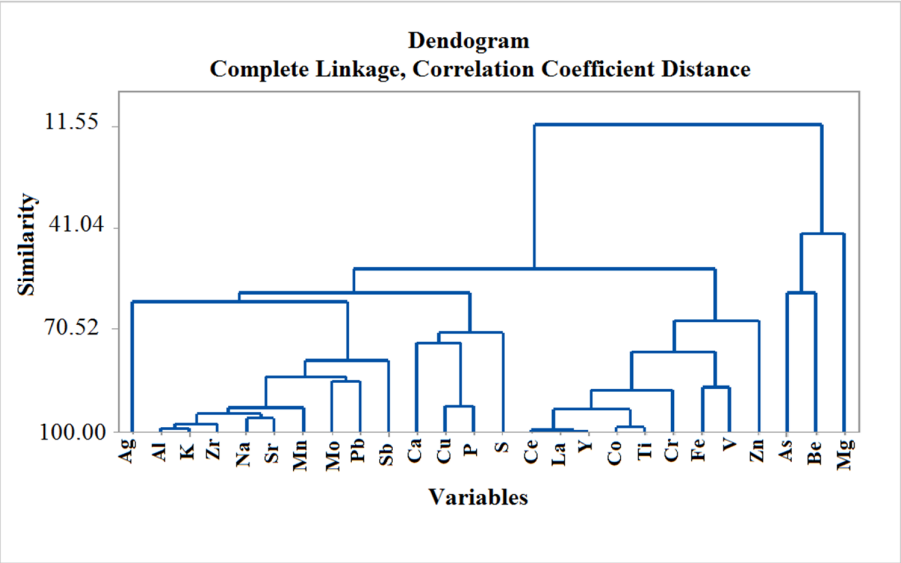

Figure 4. The dendrogram obtained from the lithogeochemical data of Qarah Tappeh

The dendrogram diagram reveals that the copper element falls within the same group as the paragenesis group of the phosphorus element. This clustering pattern is consistent with the results obtained from the factorial analysis, providing additional confirmation of the association between Cu and P in the studied geological context.

4.2. Estimating Reserves with Micromine Software

To facilitate the reserve estimation process using Micromine software, essential information is gathered, including element analysis results, borehole coordinates, borehole slope and length, and geological information. This information is then organized into Assay files, Collar, Geology, and compatible Surveys with Micromine software. In the Qarah Tappeh region, 14 exploratory boreholes, with a combined length of 909.2 meters, have been drilled. Figure 5 illustrates the positions of the drilled boreholes.

4.3. Developing a Volumetric Model for the Deposit

This geometric model, serving as a faithful representation of the deposit, is derived based on excavation data. The 3D visualization of the reserve utilizing this volumetric model proves to be highly beneficial in comprehending the geometric irregularities and mineral material displacements attributed to fault activity or other dynamic geological structures [39]. The extracted model of the study area is depicted in Figure 6.

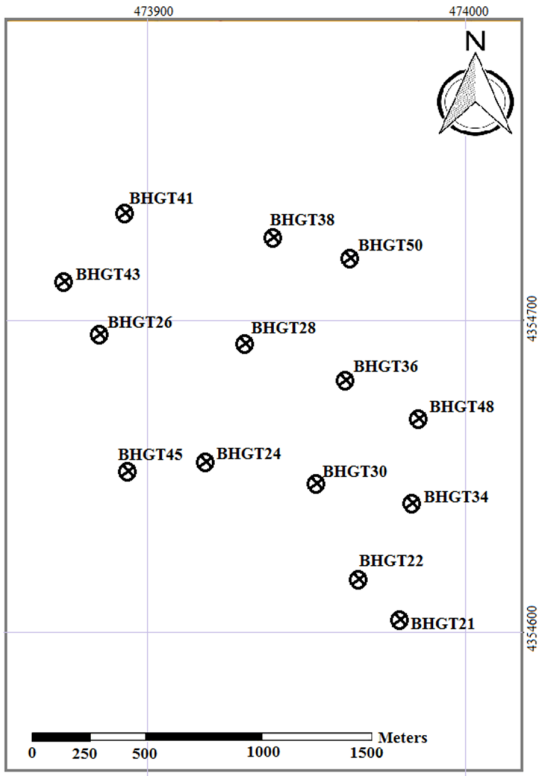

Figure 5. The position of the boreholes in the study area.

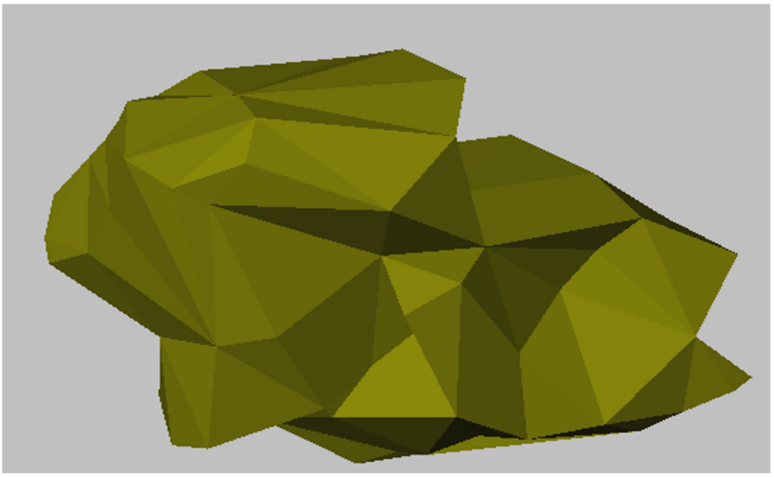

Figure 6. The volumetric model of the deposit.

4.4. Development of a Block Model for Deposit Estimation

Following the creation of the volumetric model of the deposit, the next step involves blocking the model for estimation purposes. Block dimensions are established considering the spacing between boreholes and the dimensions of the mining grid. Given the absence of an established extraction grid for the range in this project and the irregular spacing of the boreholes, block dimensions have been varied to accommodate the variations in the extent of the ranges. The extracted block model is depicted in Figure 7.

4.5. Development of a Triangulation (classic) Model for Deposit Estimation

The triangulation method is applied in cases where irregular boreholes have identified stratified deposits. This approach proves effective when the positioning of boreholes intersecting the mineral can be represented on a horizontal plane or a plane with a gentle slope. In this scenario, the midpoint of the mineral's length in each borehole is plotted on a map. At these plotted points, details such as average vertical thickness and other mineral characteristics are recorded. Subsequently, these points are interconnected to form triangles (see Figure 8, Table 3, 4). The deposit is then subdivided into prisms with the triangles as their base. The volume of these prisms is calculated, and by multiplying this volume by the average specific gravity, the ore reserve is determined [43].

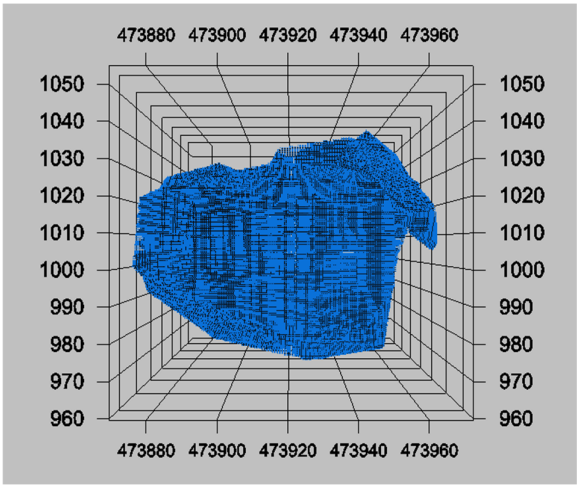

Figure 7. The block model of the deposit

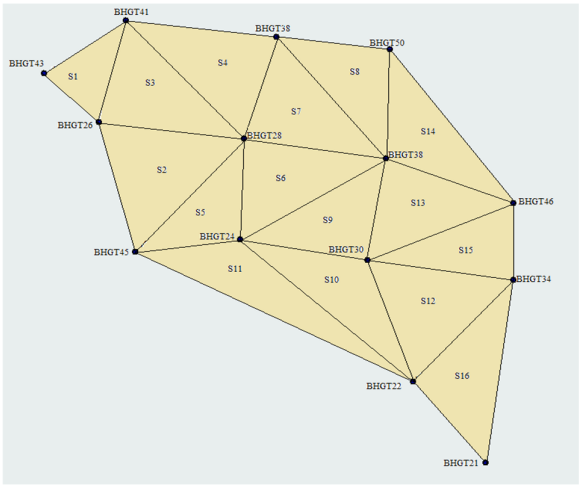

Figure 8. The formation of triangles around exploratory boreholes.

Table 3. Borehole Characteristics Employed in the Triangulation Method

Number	Drilled borehole code	The average thickness of the mineral	Cu grade (%)
A	BHGT43	24	0.1
B	BHGT26	40	0.15
C	BHGT41	26	0.08
D	BHGT38	48	0.04
E	BHGT28	73.5	0.14
F	BHGT45	22	1.97
G	BHGT24	71.8	0.32
H	BHGT36	74	0.13
I	BHGT50	62	0.02
J	BHGT48	80	0.02
K	BHGT30	84.6	0.16
L	BHGT22	92	0.32
M	BHGT34	65.5	0.13
N	BHGT21	74	0.11

Table 4. The results of reserve calculation by classical method

Tringle	S(m2)	V(m3)	W(ton)	gm (%)	P(ton)
ABC	173	4701	12999	0.11	14.3
BFE	448	18517	51200	0.45	233.3
BCE	355	14945	41324	0.13	54.4
CED	355	15809	43712	0.1	43.4
FGE	233	11867	32813	0.47	154.2
GEH	326	21581	59671	0.2	118.3
EDH	331	19558	54079	0.11	59.4
DHI	259	14411	39846	0.07	27.8
GHK	283	19678	54409	0.2	108.8
GKL	357	26812	74136	0.26	192.7
FGL	336	18991	52522	0.53	278.3
KLM	397	290475	80303	0.21	168.6
KHJ	283	18453	51019	0.11	56.12
HIJ	314	20473	56607	0.06	33.9
KJM	293	20354	56278	0.1	56.2
LMN	353	24618	68065	0.2	136.1
SUM				0.293	1390.6

4.6. Block Estimation in Kriging: Examining the Copper Grade Distribution

Kriging, a geostatistical estimation technique, encompasses point and block estimation. In the block estimation mode, the simulation involves estimating numerous points and subsequently calculating their integral. This method is typically employed in the final stages of assessing the storage of available information in a deposit, allowing for a block-by-block estimation of the deposit [39]. The block model illustrating the distribution of copper grades is depicted in Figure 9. Blocks with a light whitish color signify grades less than 0.14, those between 0.14 and 0.186, while green portions indicate grades ranging from 0.186 to 0.255. The red spectrum denotes grades from 0.255 to 0.347, and black signifies grades ranging from 0.347 to 0.37, as well as grades higher than 0.37.

Utilizing Ordinary Kriging methods on the 3D models of the deposit, volumes corresponding to various copper (Cu) grades were computed to establish a C–V fractal model. Threshold values indicative of different Cu concentrations was identified in the log–log plots of C–V, revealing a power-law relationship between Cu concentrations and corresponding volumes. The log–log plots feature arrows indicating four specific threshold values. Employing this method, mineralized zones were classified into five distinct categories: high, above-average, average, below-average, and low mineralized zones, as visually represented in Figure 10.

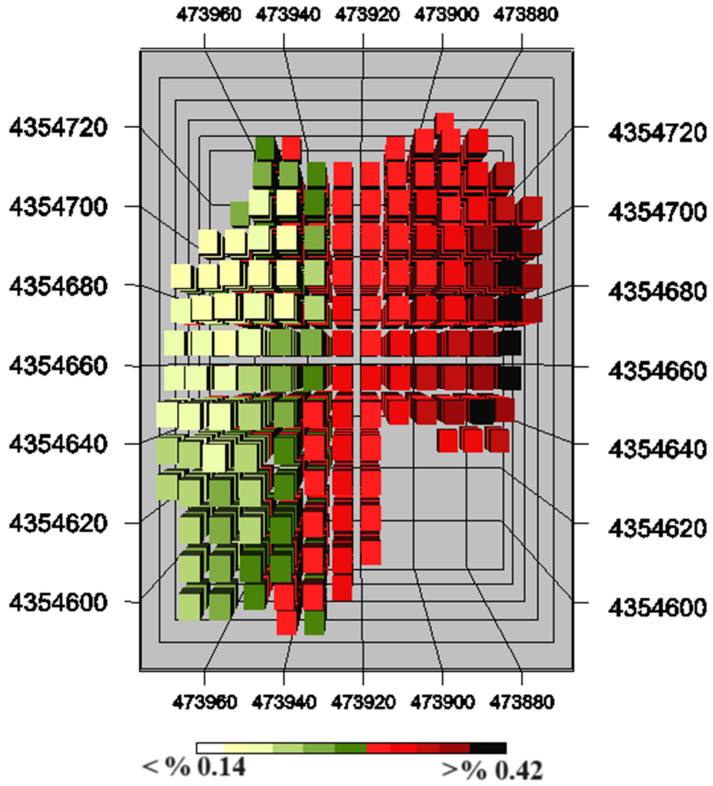

Figure 9. Block model of copper grade dispersion by geostatistical method (ordinary kriging)

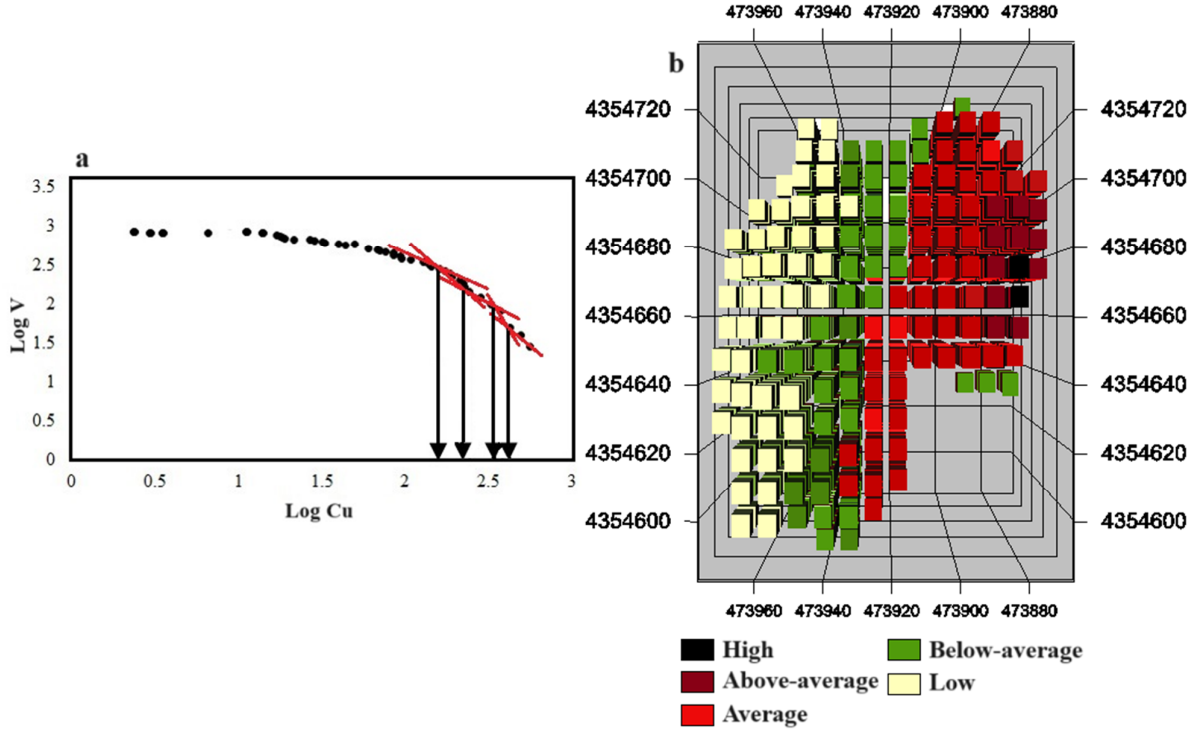

Figure 10. The C–V log–log plot for Cu concentration (a), and the separation of mineralized zones based on the thresholds extracted from the C–V fractal model by ordinary kriging (b).

5. Conclusions

The study focuses on mining highly variable vein deposits in the Qarah Tappeh area. It emphasizes the importance of careful estimation of total reserves and grade distribution to minimize risks. The study utilizes exploratory data from Qarah Tappeh's excavations, employing 3D modeling with Micromine software and ordinary kriging to assess copper reserves. Additionally, the C-V fractal method is applied to separate mineralized zones and determine grade ranges in the deposit. Overall, the aim is to enhance accuracy and reduce potential mistakes in mining operations.

The estimation plans unveiled an anisotropic and scattered mineralization process in the region, with varying characteristics among different zones. Some areas showed thick, high-grade veins, while others featured veins with low thickness or grade. The results from the normal kriging estimation method indicate a volume of 418114.8 m3, tonnage of 988604 tons, and a grade of 0.26%.

Given that the Qarah Tappeh copper mine lacks a high copper reserve and grade, the continuation of mining and exploitation in this area may not be economically viable. Identifying areas prone to new mineralization in the region is crucial.

Threshold values representing different copper (Cu) concentrations were identified through analysis of the log–log plots of the C–V relationship. The plots revealed a discernible power-law relationship between Cu concentrations and their corresponding volumes. Four specific threshold values are indicated by arrows in the log–log plots. Using this analytical approach, mineralized zones were categorized into five distinct classes: high (>0.42%), above-average (0.35-0.42%), average (0.27-0.35%), below-average (0.14-0.27%), and low (<0.14%) mineralized zones.

References

[1]. Turcotte, D. L., & Newman, W. I. (1996). Symmetries in geology and geophysics. *Proceedings of the National Academy of Sciences*, *93*(25), 14295-14300.

[2]. Cheng, Q., Agterberg, F. P., & Ballantyne, S. B. (1994). The separation of geochemical anomalies from background by fractal methods. *Journal of Geochemical exploration, 51*(2), 109-130.

[3]. Hassanpour, S., & Afzal, P. (2013). Application of concentration–number (C–N) multifractal modeling for geochemical anomaly separation in Haftcheshmeh porphyry system, NW Iran. *Arabian Journal of Geosciences, 6*, 957-970.

[4]. Barak, S., Bahroudi, A., & Jozanikohan, G. (2017). Exploration of neysian area by geochemical data and fractal concentration-number (CN). *In National Conference on Science, Engineering* (pp. 1-10).

[5]. Barak, S., Bahroudi, A., & Jozanikohan, G. (2018). Exploration of Kahang porphyry copper deposit using advanced integration of geological, remote sensing, geochemical, and magnetics data. *Journal of Mining and Environment, 9*(1), 19-39.

[6]. Barak, S., Bahroudi, A., & Jozanikohan, G. (2018). The use of fuzzy inference system in the integration of copper exploration layers in Neysian. *Journal of Mining Engineering, 13*(38), 97-112.

[7]. Barak, S., Imamalipour, A., Abedi, M., Bahroudi, A., & Khalifani, F. M. (2021). Comprehensive modeling of mineral potential mapping by integration of multiset geosciences data. *Geochemistry, 81*(4), 125824.

[8]. Barak, S., Imamalipour, A., & Abedi, M. (2023). Application of Fuzzy Gamma Operator for Mineral Prospectivity Mapping, Case Study: Sonajil Area. *Journal of Mining and Environment, 14*(3), 981-997.

[9]. Barak, S., Abedi, M., & Yousefi, S. (2023). Gold prospectivity mapping through generation and integration of geophysical, geochemical, remote sensing, and geological evidence layers in Saqez area, NW Iran. *International Journal of Mining & Geo-Engineering, 57*(4).

[10]. Khalifani, F. M., Imamalipour, A., Barak, S., Abedi, M., Jozanikohan, G., & Bahroudi, A. (2023). The application of various mineral prospectivity modeling in the exploration of orogenic gold deposit in Saqez-Sardasht region, northwest Iran. *Lithology and Mineral Resources, 58*(4), 368-386.

[11]. Yasrebi, A. B., Afzal, P., Wetherelt, A., Foster, P. J., & Esfahanipour, R. (2013). Correlation between geology and concentration-volume fractal models: significance for Cu and Mo mineralized zones separation in the Kahang porphyry deposit (Central Iran).

[12]. Afzal, P., Madani, N., Shahbeik, S., & Yasrebi, A. B. (2015). Multi-Gaussian kriging: a practice to enhance delineation of mineralized zones by Concentration–Volume fractal model in Dardevey iron ore deposit, SE Iran. *Journal of Geochemical Exploration, 158*, 10-21.

[13]. Khalili, H., & Afzal, P. (2018). Application of spectrum-volume fractal modeling for detection of mineralized zones. *Journal of Mining and Environment, 9*(2), 371-378.

[14]. Shokouh Saljoughi, B., Hezarkhani, A., & Farahbakhsh, E. (2018). A comparative study of fractal models and U-statistic method to identify geochemical anomalies; case study of Avanj porphyry system, Central Iran. *Journal of Mining and Environment, 9*(1), 209-227.

[15]. Nikoogoftar Safa, H., & Hezarkhani, A. (2019). Application of fractal modeling to delineate alteration zones and lithological units in Masjed-Daghi Cu-Au porphyry deposit, NW Iran. *Journal of Mining and Environment, 10*(2), 339-356.

[16]. Gholampour, O., Hezarkhani, A., Maghsoudi, A., & Mousavi, M. (2019). Delineation of alteration zones based on kriging, artificial neural networks, and concentration–volume fractal modelings in hypogene zone of Miduk porphyry copper deposit, SE Iran. *Journal of Mining and Environment, 10*(3), 575-595.

[17]. Salarian, S., Asghari, O., Abedi, M., & Alilou, S. K. (2019). Geostatistical and multi-fractal modeling of geological and geophysical characteristics in Ghalandar Skarn-Porphyry Cu Deposit, Iran. *Journal of Mining and Environment, 10*(4), 1061-1081.

[18]. Lotfi, M., & Tokhmechi, B. (2019). Fractal-wavelet-fusion-based re-ranking of joint roughness coefficients. *Journal of Mining and Environment, 10*(4), 1121-1133.

[19]. Khojamli, A., Doulati Ardejani, F., Moradzadeh, A., Nejati Kalateh, A., Roshandel Kahoo, A., & Porkhial, S. (2017). Determining fractal parameter and depth of magnetic sources for Ardabil geothermal area using aeromagnetic data by de-fractal approach. *Journal of Mining and Environment, 8*(1), 93-101.

[20]. Aliyari, F., Afzal, P., & Abdollahi Sharif, J. (2017). Determination of geochemical anomalies and gold mineralized stages based on litho-geochemical data for Zarshuran Carlin-like gold deposit (NW Iran) utilizing multi-fractal modeling and stepwise factor analysis. *Journal of Mining and Environment, 8*(4), 593-610.

[21]. Saljoughi, B. S., & Hezarkhani, A. (2020). Delineation of Alteration Zones Based on Wavelet Neural Network (WNN) and Concentration–Volume (CV) Fractal Methods in the Hypogene Zone of Porphyry Copper Deposit, Shahr-e-Babak District, SE Iran. *Journal of Mining and Environment, 11*(4), 1173-1190.

[22]. Mahdiyanfar, H., & Salimi, A. (2022). Fractal Modeling of Geochemical Mineralization Prospectivity Index based on Centered Log-Ratio Transformed Data for Geochemical Targeting: a Case Study of Cu Porphyry Mineralization. *Journal of Mining and Environment, 13*(3), 821-838.

[23]. Mahdiyanfar, H., & Seyedrahimi-Niaraq, M. (2023). Integration of Fractal and Multivariate Principal Component Models for Separating Pb-Zn Mineral Contaminated Areas. *Journal of Mining and Environment, 14*(3), 1019-1035.

[24]. Qaderi, A. (2019). Feasibility study of ipcc conveyor system in Haji Abad Bukan mine, Master's thesis in mining engineering. Urmia University.

[25]. Gholami, S. (2017). Determining the limit grade, designing the final range and planning the optimal production of Qalqeleh gold mine (southwest Saqez) using the latest exploration data. Master's thesis in mining engineering. Urmia University.

[26]. Azarnia, Z. (2019). Providing an approach for geological and block modeling of decorative stone deposits in order to increase productivity (case study: Qaragheshlaq marble deposit). Master's thesis in mining engineering. Urmia University.

[27]. Akbar, D. A. (2012). Reserve estimation of central part of Choghart north anomaly iron ore deposit through ordinary kriging method. *International Journal of Mining Science and Technology, 22*(4), 573-577.

[28] Lloyd, C. D., & Atkinson, P. M. (2001). Assessing uncertainty in estimates with ordinary and indicator kriging. *Computers & Geosciences, 27*(8), 929-937.

[29]. Mostafaei, K., & Ramazi, H. (2019). Investigating the applicability of induced polarization method in ore modelling and drilling optimization: a case study from Abassabad, Iran. *Near Surface Geophysics, 17*(6-Recent Developments in Induced Polarization), 637-652.

[30]. Mostafaei, K., & Ramazi, H. (2019). Mineral resource estimation using a combination of drilling and IP-Rs data using statistical and cokriging methods. *Bulletin of the mineral research and exploration, 160*(160), 177-195.

[31]. Goodarzi, A. (2013). Estimation of Jian Buanat copper deposit using geostatistical and fractal methods, Master's thesis in Mining Engineering. Isfahan University.

[32]. Aghazadeh, V., & Nabizadeh, A. (2015). Study and Suitable Method Selection for Copper Leaching from Its Oxide Ore: Case Study of Ghare Tappeh Copper Ore. *Journal of Mining Engineering, 10*(28), 35-42.

[33]. Dareh, F., Hosseinzadeh, M. R., & Movid, M. (2013). Economic Geology of Qarah Tappeh Copper Indices (Maku - West Azerbaijan), *sixth Conference of Economic Geology Association of Iran*, Zahedan.

[34]. Karami, K., & Afzal, P. (2015). Application of multifractal modeling for separation of sulfidic mineralized zones based on induced polarization and resistivity data in the Ghare-Tappeh Cu deposit, NW Iran. *Iranian Journal of Earth Sciences, 7*(2), 134-141.

[35]. KanKav Consulting Engineers Company. (2013). The final report of conducting exploration operations in the copper mining area of Qarah Tappeh Maku.

[36]. Aghanabati, S. A. (2004). Geology of Iran. *Geological Survey and Mining Exploration of Iran*, Tehran. 586p.

[37]. Majidzadeh, M., & Najafabadi, M. (2014). Exploration, design and extraction of open pit mines

with the approach of using software in iron ore mines. Jihad University Press.

[38]. Hasani Pak, A. A., & Sharafaddin, M. (2001). Exploration data analysis. Tehran University Press.

[39]. Yekani Moltaq, Z. (2018). three-dimensional geochemical modeling, reserve evaluation and element concentration prediction by smart method in gold-zinc prospecting area of Dagh Dali, North Takab. Master's thesis of Mining Engineering. Urmia University.

[40]. Afzal, P., Alghalandis, Y. F., Khakzad, A., Moarefvand, P., & Omran, N. R. (2011). Delineation of mineralization zones in porphyry Cu deposits by fractal concentration–volume modeling. *Journal of Geochemical exploration, 108*(3), 220-232.

[41]. Carranza, E. J. M. (2008). Geochemical anomaly and mineral prospectivity mapping in GIS. Elsevier.

[42]. Barak, S., Bahroudi, A., Jozani, G., & Aslani, S. (2016). The geochemical anomaly separation by using the soil samples of eastern of Neysian, Isfahan Province. *Geochemistry*, 5(1), 55-71.

[43]. Sinclair, A. J., & Blackwell, G. H. (2006). Applied mineral inventory estimation. Cambridge University Press.

کاربرد مدلسازی فراکتال برای برآورد دقیق منابع در کانسار مس قره تپه شمال غرب ایران

سپیده قاسمی[۱]، علی امامعلی‌پور[۱*] و سمانه برک

۱- گروه مهندسی معدن، دانشکده فنی و مهندسی، دانشگاه ارومیه، ایران

ارسال ۲۰۲۳/۰۹/۱۳، پذیرش ۲۰۲۳/۰۴/۱۲

* نویسنده مسئول مکاتبات: a.imamalipour@urmia.ac.ir

چکیده:

این تحقیق بر روی کانسار مس قره تپه واقع در شمال استان آذربایجان غربی و در فاصله تقریبی ۱۵ کیلومتری شمال شرق شهرستان ماکو متمرکز است. هدف اصلی این مطالعه، بررسی جامع منطقه مورد مطالعه از طریق تجزیه و تحلیل ۲۵۳ نمونه لیتوژئوشیمیایی، و ارزیابی ذخایر با استفاده از کریجینگ معمولی، هدایت داده‌های زیرسطحی به‌دست‌آمده از ۱۴ گمانه به طول ۹۰۹.۲ متر است. رویکرد مدل‌سازی چندفراکتالی غلظت-حجم (C-V) برای تخمین ذخیره سپرده مورد استفاده قرار گرفت. یافته های این پروژه تحقیقاتی حاکی از برآورد ۹۸۸۶۰۴ تن کانسار با عیار متوسط ۰.۱۴ درصد است. از طریق تجزیه و تحلیل نمودارهای ورود به سیستم در رابطه C-V، مقادیر آستانه نشان دهنده غلظت های مختلف مس (مس) شناسایی شد. این نمودارها یک همبستگی قوی-قانونی را بین غلظت مس و حجم متناظر آن‌ها با فلش‌هایی که چهار مقدار آستانه خاص را نشان می‌دهند، نشان دادند. با استفاده از این روش تحلیلی، پهنه های معدنی به پنج دسته متمایز طبقه بندی شدند: بالا (>۰.۴۲٪)، بالاتر از میانگین (۰.۳۵-۰.۴۲٪)، متوسط (۰.۲۷-۰.۳۵٪)، زیر متوسط (۰.۱۴-۰.۲۷٪) و زون‌های کم معدنی (<۰.۱۴٪).

کلمات کلیدی: فراکتال، تخمین ذخیره، کریجینگ معمولی، میکرومین، کانسار مس قره تپه.